Designing Mirrors for Catadioptric Systems that Minimize Image Errors*

Rahul Swaminathan[1], Michael D. Grossberg[2], and Shree K. Nayar[2]

[1] GRASP Lab, Univ. Of Pennsylvania, Philadelphia PA 19104, USA
[2] Columbia University, New York NY 10027, USA
srahul@grasp.cis.upenn.edu

Abstract

A critical step in designing any catadioptric system is determining the shape of its component mirrors. Many mirror shapes have been designed in the past for numerous applications. Invariably these mirrors were designed using case specific tools and required considerable effort on the part of the designer. Recently, some new general methods have been developed to automate the design process. However, all previous approaches determined the mirror by minimizing errors in the mirror shape rather than the image formed. A more principled formulation is to instead determine a mirror that reduces geometric errors in the images that the system produces. In general, such a formulation makes the problem non-linear and computationally prohibitive.

In this paper we present a linear method to determine the mirror shape that meets a designer's requirements. The requirements are specified as a map from pixels to scene points which we call the *image-to-scene map*. For the case when an exact solution for the mirror shape does exist, our method finds it. A more interesting and common case is when no mirror shape exists that implements the required map. In this case, our method finds the mirror shape that minimizes geometric errors in image formation. The method achieves this by relating the errors in the mirror normals to a first-order approximation of image errors. We show how the constraints of a previous shape based methods can be modified so as to minimize image errors. Our proposed method is also directly applicable to the design of projection systems. We demonstrate the effectiveness of our approach on various catadioptric imaging and projection systems showing up to an 80 percent reduction in errors with respect to previous shape based methods.

* This research was conducted at the Columbia Vision and Graphics Center in the Computer Science Department at Columbia University. It was supported in parts by an NSF ITR Grant (IIS-00-85864) and a DARPA HID Contract (No. N00014-00-1-0929).

1 Design of Catadioptric Systems

Recent years have seen a growing interest in the design and use of many non-conventional imaging systems. These imaging systems are better suited than conventional perspective imaging systems for many applications including surveillance and navigation. For instance, acquiring a 360 degree panoramic video with a single perspective camera is impossible. However, with specially designed optics, this can be easily achieved. Recognizing this fact, many non-conventional imaging systems which use both lenses and mirrors (catadioptric systems) have been proposed.

The most common use of catadioptric imaging is to enhance the field of view. Systems that achieve this goal have been developed using both planar as well as curved mirrors. Some of these systems have been designed to have a single effective viewpoint [1–6]. Other systems have been designed to achieve specific resolution characteristics, such as the equi-angular mapping[7], the constant-resolution mapping[8] and the equi-areal mapping[9]. Systems have also been designed to acquire images of a known scene in special ways[10–17].

A critical aspect of designing a catadioptric imaging system is determining the appropriate shapes of the one or more mirrors that the system uses.[3] Let us consider a system that has a single mirror. To determine the shape of this mirror, we assume that the *primary optics* (perspective lens, telecentric lens or otherwise) is known. We also assume that the system requirements are specified by the designers as a map from pixels in the image to scene points or viewing directions, which we refer to as the *image-to-scene map*. Halstead et al were the first to use this formulation for the related problem of recovering the shape of specular surfaces using perspective imaging systems [20]. Hicks and Perline later reposed the problem for *mirror design* in terms of the image-to-scene map. They also proposed the use of "geometric distributions" to test for the existence of a mirror shape that implements the given image-to-scene map.

The mirror for each of the systems designed previously was found using constraints imposed by the image-to-scene map to derive partial differential equations (PDEs) that the mirror must satisfy. The mirror shape was then determined by finding solutions to the resulting PDEs. This approach requires considerable skill and effort on the part of the designer. In contrast, the spline based technique in [20] is better suited for automatic mirror design without human effort. In [21] we extended their method using a splines based formulation to also include non-perspective cameras[21].

An important case to consider when designing mirrors is when there may not exist a single mirror that exactly implements the required image-to-scene map. In such cases, all the methods described above determine a mirror surface that minimizes errors in its three-dimensional shape (errors in the orientations

[3] In general, the performance of an imaging system has two components. One is its ability to adhere to the prescribed image-to-scene map and the second is its optical image quality (determined by depth of field, coma, astigmatism, etc. [18, 19]). This paper focuses on the first of these components.

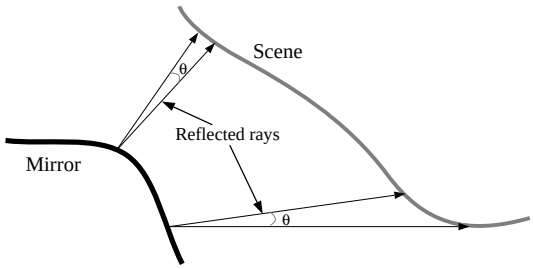

Figure 1. The normal at two points on the mirror is perturbed by equally. Assuming parallel incident rays, the reflected rays will be perturbed equally by θ as shown. As can be seen, this causes unequal scene errors and therefore unequal image errors. A mirror designed to minimize errors in the orientation of the normal, therefore does not necessarily minimize image errors.

of surface normals). However, as shown in Fig.1, a mirror that minimizes errors in its normals *need not minimize image errors*. That is, the resulting mirror may have normals that are close to the desired set of normals but produces very large distortions in the captured image. Since we are interested in the geometric quality of the image captured by the imaging system, the correct approach is to find a mirror that minimizes image errors.

Note that a method for designing mirrors for imaging can also be used to design projection systems. In this case, the mirror must minimize scene projection errors. In general, minimizing either the image error or scene error requires a non-linear optimization, which can be highly unstable. In [21], we recognized this problem and addressed it by using a heuristic weighting approach. However, this technique does not accurately model either image or scene errors and hence does not guarantee good solutions.

In this work, we derive first-order approximations to image and scene errors. We incorporate these approximations into the algorithm in [21] to determine the mirror shape that minimizes image or scene errors, without the need for a costly non-linear optimization. We present experimental results to demonstrate the effectiveness of such an approach.

2 Spline-Based Mirror Design

We assume that the catadioptric system being designed consists of some *known primary optics* and an *unknown mirror*. The imaging specifications are assumed to be provided by the designer in terms of a map from pixels in the image to points in the scene. We call this the *image-to-scene* map which we denote $\mathcal{M}(u, v)$. Our goal is to find the mirror which in combination with the known primary optics implements the desired image-to-scene map $\mathcal{M}$.

A general approach to finding mirror shapes was provided by Halstead et al using tensor splines in the context of specular surface recovery [20]. In our previous work, we applied an equivalent formulation of this shape based technique to

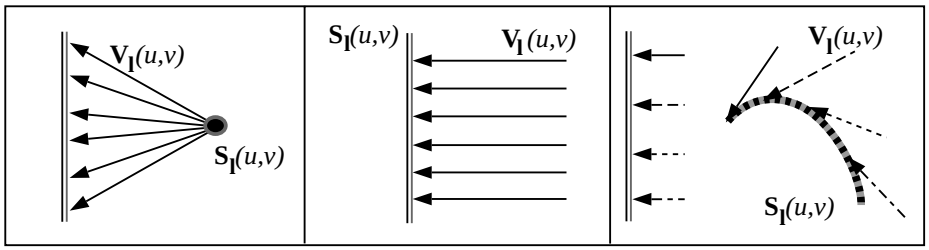

Figure 2. Models of the primary optics for which our method can compute a mirror shape. (a) Perspective projection, using conventional imaging systems. (b) Orthographic projection, typically obtained with telecentric lenses. (c) The generalized imaging model, wherein each pixel can have its own associated viewpoint and viewing direction providing greater flexibility to the designer.

the problem of mirror design. Our emphasis in this work however, is to modify the equations used in [21] so that the mirror we compute minimizes image or scene errors. We begin by briefly describing the previous shape based method in order to define the notation we use. Throughout this paper we will address the problem of catadioptric imaging system design. However, the same analysis can be directly applied to projector design as well.

2.1 Modeling the Primary Optics

The *primary optics* of the catadioptric system could either use a conventional lens (perspective projection) as in Fig. 2(a), or a telecentric lens (orthographic projection) as shown in Fig. 2(b), or any general imaging system [22] (see Fig. 2(c)), where any pixel (u, v) in the image possesses a viewpoint $\mathbf{S_l}(u, v)$ and a viewing direction $\mathbf{V_l}(u, v)$. This general model provides greater flexibility to the designer of the imaging system. This is critical because for certain image-to-scene maps, a mirror may exist only with one type of primary optics and not with another. Furthermore, the generality also allows for the design of compound catadioptric systems that employ multiple mirrors [23].

2.2 Modeling the Mirror Shape

As in [21], we express the mirror shape $\mathbf{S_r}$, using the primary optics model, as:

$$\mathbf{S_r}(u, v) = \mathbf{S_l}(u, v) - D(u, v)\mathbf{V_l}(u, v), \tag{1}$$

where $D(u, v)$ is the distance of the mirror from the viewpoint surface. We model $D(u, v)$ using the *tensor product spline* as:

$$D(u, v) = \sum_{i=1}^{K_f} \sum_{j=1}^{K_g} c_{i,j} f_i(u) g_j(v), \tag{2}$$

where $f_i(u)$ and $g_j(v)$ are 1-D spline basis functions, $c_{i,j}$ are the coefficients of the spline model, and $K_f \cdot K_g$ are the number of spline coefficients.

2.3 Mirror Normal Equations

Fig. 3 shows a catadioptric system used to image some known scene. The mirror surface $\mathbf{S_r}(u,v)$ must implement the user provided image-to-scene mapping $\mathcal{M}$ by reflecting each scene point $\mathcal{M}(u,v)$ along the scene ray $\mathbf{V_r}(u,v)$ into the primary optics, where:

$$\mathbf{V_r}(u,v) = \frac{\mathbf{S_r}(u,v) - \mathcal{M}(u,v)}{|\mathbf{S_r}(u,v) - \mathcal{M}(u,v)|}. \tag{3}$$

This constrains the surface normal of the mirror $\mathbf{N_r}$ as:

$$\mathbf{N_r}(u,v) = \frac{\mathbf{V_l}(u,v) - \mathbf{V_r}(u,v)}{|\mathbf{V_l}(u,v) - \mathbf{V_r}(u,v)|}. \tag{4}$$

The tangent vectors $\mathbf{T}_u(u,v) = \frac{\partial \mathbf{S_r}(u,v)}{\partial u}$ and $\mathbf{T}_v(u,v) = \frac{\partial \mathbf{S_r}(u,v)}{\partial v}$ on the mirror surface must be orthogonal to the normal in Eq.(4). This provides two constraints on the mirror shape:

$$\begin{aligned} \mathbf{T}_u(u,v) \cdot \mathbf{N_r}(u,v) &= 0, \\ \mathbf{T}_v(u,v) \cdot \mathbf{N_r}(u,v) &= 0. \end{aligned} \tag{5}$$

In [20, 21], the above constraints are used to present an iterative algorithm, that determines the mirror shape. This shape however minimizes the errors in orientation of normal vectors. However, minimizing the error in the shape of

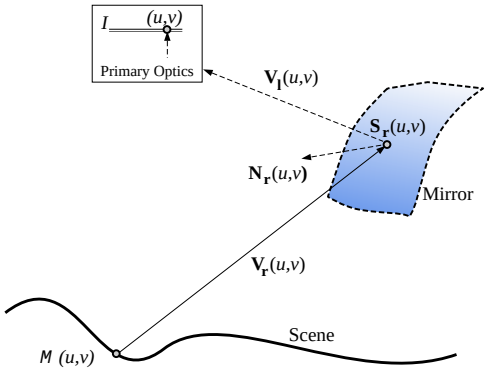

Figure 3. A catadioptric imaging system consisting of some known primary optics and a mirror. In general, a pixel (u,v) in the image maps to the scene point $\mathcal{M}(u,v)$ after reflecting at $\mathbf{S_r}(u,v)$ on the mirror. This forces linear constraints on the surface normals $\mathbf{N_r}(u,v)$ of the mirror.

the mirror does not, in general, result in creating an image with the smallest geometric error. In terms of imaging system design, it is imperative to compute the mirror shape that minimizes errors in the image, while preserving linearity of the constraints from Eq.(5).

3 Reducing Scene and Image Error

We now present a simple method to estimate the mirror shape that approximately minimizes image or scene projection errors. Before doing so however, we need to define scene error and image errors.

Consider a catadioptric system that must implement some image-to-scene map $\mathcal{M}(u, v)$. When no mirror shape exists that can exactly implement $\mathcal{M}(u, v)$, the mirror shape is approximate. Therefore a light ray corresponding to pixel (u, v) gets reflected towards a scene point other than the required point $\mathcal{M}(u, v)$. Let $\eta(u, v)$ be the effective (possibly erroneous) image-to-scene map that the catadioptric system with a given mirror implements. The scene error ξ_ρ at a point (u, v) is then given by:

$$\xi_\rho = |\eta(u, v) - \mathcal{M}(u, v)|. \tag{6}$$

For an imaging system, the image error can be computed by simply inverse mapping the effective scene point $\eta(u, v)$ onto the image using the ideal image-to-scene map $\mathcal{M}(u, v)$. The image error ξ_I at pixel (u, v) is:

$$\xi_I = |\mathcal{M}^{-1}(\eta(u, v)) - (u, v)|. \tag{7}$$

When an exact mirror shape exists, the errors ξ_I, ξ_ρ and Eqs.(5) all vanish. When no mirror shape exists that implements the desired image-to-scene map, the Eqs. (5) are not satisfied and can be rewritten as:

$$\xi_O = \begin{pmatrix} \xi_{O,u} \\ \xi_{O,v} \end{pmatrix} = \begin{pmatrix} \mathbf{T}_u \cdot \mathbf{N_r} \\ \mathbf{T}_v \cdot \mathbf{N_r} \end{pmatrix} \tag{8}$$

where $\xi_{O,u}$ and $\xi_{O,v}$ denote the residues corresponding to the two constraint equations respectively.

The least squares solution of Eqs. (5) minimizes the mean square of the residual ξ_O. Our goal is to formulate linear equations whose least square solutions better approximate the image or scene errors. To do so, we first derive a relationship between the residual and angular perturbations of the tangent vectors. Next we relate the angular tangent perturbations to errors in the reflected rays and thus scene errors. The last step is to relate the scene errors to image errors.

3.1 Relating Angular Perturbations of Tangents to Residuals

Referring to Eq. (1) for the mirror shape, the surface tangents are given by $\mathbf{T}_u = \frac{\partial \mathbf{S_r}}{\partial u}$ and $\mathbf{T}_v = \frac{\partial \mathbf{S_l}}{\partial u}$ respectively. Taking tangent $\mathbf{T}_u$ into consideration, we first note that it can be rewritten as:

$$\mathbf{T}_u = \frac{\partial D}{\partial u}\mathbf{V_l} + \left(D\frac{\partial \mathbf{V_l}}{\partial u} - \frac{\partial \mathbf{S_l}}{\partial u} \right). \tag{9}$$

For a given pixel (u, v), the quantities $\frac{\partial \mathbf{V_l}}{\partial u}$ and $\frac{\partial \mathbf{S_l}}{\partial u}$ depend on the primary optics and are independent of the mirror shape (tensor-spline coefficients). In analyzing the perturbations of the tangents we consider the location of a point on the mirror $\mathbf{S_r}(u, v)$ to be essentially fixed. Thus, $D(u, v)$ changes slowly with respect to changes in the spline coefficients. The variation in tangents with respect to the coefficients is thus almost entirely due to changes in $\frac{\partial D(u,v)}{\partial u}$. This restricts $\mathbf{T}_u$ to a plane $\mathcal{P}_u$ spanned by the vectors $\mathbf{V_l}$ and $D\frac{\partial \mathbf{V_l}}{\partial u} - \frac{\partial \mathbf{S_l}}{\partial u}$. Thus, perturbations to $\mathbf{T}_u$ can be expressed simply as a rotation in this plane.

Let $\pi_u(\mathbf{N_r})$ be the projection of $\mathbf{N_r}$ onto the plane $\mathcal{P}_u$. We note that the component of $\mathbf{N_r}$ which is orthogonal to plane $\mathcal{P}_u$ is automatically orthogonal to $\mathbf{T}_u$. Therefore this component of $\mathbf{N_r}$ is irrelevant. We can then express the angle θ_u between $\pi_u(\mathbf{N_r})$ and $\mathbf{T}_u$ in terms of the residual as:

$$\cos\theta_u = \xi_{O,u}/(|\mathbf{T}_u||\pi_u(\mathbf{N_r})). \tag{10}$$

Similarly, $\xi_{O,v}$ can be related to θ_v as

$$\cos\theta_v = \xi_{O,v}/(|\mathbf{T}_v||\pi_v(\mathbf{N_r})). \tag{11}$$

The angles (θ_u, θ_v) specify the directions of the tangents for a given iteration. We write the first order approximation for a perturbation of these angles by $(\Delta\theta_u, \Delta\theta_v)$ as:

$$\begin{pmatrix} \Delta\theta_u \\ \Delta\theta_v \end{pmatrix} \approx \begin{pmatrix} \cot(\theta_u) \\ \cot(\theta_v) \end{pmatrix} - L \begin{pmatrix} \xi_{O,u} \\ \xi_{O,v} \end{pmatrix} \tag{12}$$

where L is a diagonal matrix with diagonal elements

$$\begin{aligned} L_1 &= -1/\sin(\theta_u)|\mathbf{T}_u||\pi_{\alpha_u}(\mathbf{N_r})| \\ L_2 &= -1/\sin(\theta_v)|\mathbf{T}_v||\pi_{\alpha_v}(\mathbf{N_r})| \end{aligned} \tag{13}$$

The quantity $\pi_u(\mathbf{N_r})$ can be computed at every iteration of our method and does not depend on the unknown tangents. The length $|\mathbf{T}_u|$ does depend on the unknown tangents. However, in our iterative method to determine the mirror shape, we find that $|\mathbf{T}_u|$ remains relative constant across iterations. The reasons for this can be seen in Eq. (9). As already noted, $\mathbf{T}_u$ is a sum of three terms with $\frac{\partial \mathbf{S_l}}{\partial u}$ constant for each iteration and with $D\frac{\partial \mathbf{V_l}}{\partial u}$ changing slowly because it depends only on the mirror position.

So far we derived a first order relationship between the residuals of the constrains of Eqs. (5) and perturbations of the tangent vectors. We shall use this relationship next to determine the scene errors.

3.2 Relating Scene Error to Residuals

We now present our method of relating tangent perturbations to scene errors. This will be used to modify Eqs. (5) in order to approximate the scene errors.

The three dimensional vector which represents the scene error is:

$$\xi_\rho = (\xi_{\rho,x}, \xi_{\rho,y}, \xi_{\rho,z}) = \eta(u, v) - M(u, v). \tag{14}$$

For a given pixel we consider the vector scene error ξ_ρ as a function of the angles θ_u and θ_v. The first order approximation of the vector scene error due to angular perturbations $\Delta\theta_u$ and $\Delta\theta_v$ is then given by:

$$\begin{pmatrix} \xi_{\rho,x}(\theta_u,\theta_v) \\ \xi_{\rho,y}(\theta_u,\theta_v) \\ \xi_{\rho,z}(\theta_u,\theta_v) \end{pmatrix} + J(\xi_\rho) \begin{pmatrix} \Delta\theta_u \\ \Delta\theta_v \end{pmatrix} \tag{15}$$

where $J(\xi_\rho)$ is the Jacobian, given by:

$$J(\xi_\rho) = \begin{pmatrix} \frac{\partial \xi_{\rho,x}}{\partial u} & \frac{\partial \xi_{\rho,x}}{\partial v} \\ \frac{\partial \xi_{\rho,y}}{\partial u} & \frac{\partial \xi_{\rho,y}}{\partial v} \\ \frac{\partial \xi_{\rho,z}}{\partial u} & \frac{\partial \xi_{\rho,z}}{\partial v} \end{pmatrix}. \tag{16}$$

When the angles of the tangent vectors of the mirror $\mathbf{T}_u$ and $\mathbf{T}_v$ are perturbed by a small amount $\Delta\theta_u$ and $\Delta\theta_v$ about $\pi/2$, the cotangent term in Eq. (12) vanishes and $\sin(\pi/2) = 1$ in Eq. (13). Combining these equations with Eq. (15) we have the first order approximation for scene error as

$$\xi_\rho \approx J(\xi_\rho) L \xi_O. \tag{17}$$

Observe from Eq. (5) that the residuals ξ_O are given by a pair of linear equations in the spline coefficients for each pixel. We multiply each pair of equations from the left by the 3×2 matrix $J(\xi_\rho)L$ to obtain three linear equations in the spline coefficients. A least squares solution of these modified linear equations approximates the minimization of the scene error to first order. These are the equations we use to compute the mirror shape for catadioptric projection systems.

3.3 Relating Image Error to Residuals

For imaging systems we wish to minimize the image error defined in Eq. (7). This can be achieved by mapping the scene errors back to the image using the inverse $\mathcal{M}^{-1}$ of the image-to-scene map. However, since the Jacobian of the image-to-scene map $J(\mathcal{M})$ is a 3×2 matrix, we employ a left pseudo-inverse to transform the scene error to the image error as

$$\xi_I \approx (J(\mathcal{M})^T J(\mathcal{M}))^{-1} J(\mathcal{M})^T J(\xi_\rho) \xi_\rho. \tag{18}$$

Combining this with Eq. (17), a first order approximation for image error is then:

$$\xi_I \approx ((J(\mathcal{M})^T J(\mathcal{M}))^{-1} J(\mathcal{M})^T J(\xi_\rho) L \xi_O. \tag{19}$$

Hence, we now have a simple method to transform the residuals in Eqs. (5) into the image or scene error. To do so, we simply multiply the constraint equations by an appropriate transformation matrix as in Eqs. (17,19). This results in a new set of linear equations that approximate, to first order, the minimization of the scene or image error respectively.

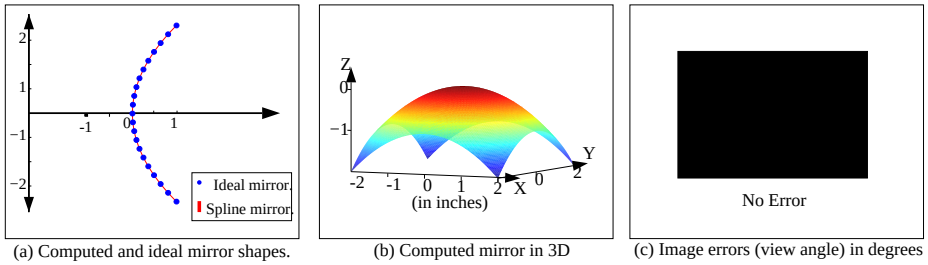

(a) Computed and ideal mirror shapes. (b) Computed mirror in 3D (c) Image errors (view angle) in degrees

Figure 4. Results of applying our general mirror design method to a para-catadioptric imaging system. (a, b) The mirror shape computed is identical to the ground truth shape demonstrating that our method produces (c) error free solutions for cases when a mirror exists for the prescribed image-to-scene map.

4 Experimental Verification

We now present resulting mirror shapes for various systems computed using our image or scene error minimizing approach. We begin with the example of a single viewpoint para-catadioptric camera [5]. Next we present two new designs for different imaging scenarios. One is a conference table as described in [21] and the other a projection system for immersive viewing within a spherical screen.

4.1 Single Viewpoint Sensors

We computed the mirror for a para-catadioptric [5] imaging system using a telecentric lens for the primary optics (orthographic projection). The mirror was designed by specifying an image-to-scene map such that all the imaged rays pass through a virtual viewpoint located $1cm$ below the apex of the reflector. As seen in Fig. 4(a), the profile of the computed mirror using our method matches precisely with the analytically derived parabolic profile. The resulting $3D$ mirror shape and the zero image errors are also shown in Fig. 4(b,c). This example is important because it demonstrates that our method produces an error free solution for mirrors for which a solution exists.

4.2 Conference Table Rectification

We now consider a video conferencing scenario where people seated at a conference table are imaged. We would like to display the acquired image directly, such that the curved edge of the table appears straight and all the people appear to be the same size as if seated along a desk. Fig. 5(a) shows the setup of such an imaging system (similar to [21]). The computed mirror shape and corresponding errors are illustrated in Figs. 5(b,c). We also compare our method against an hypothetical ideal sensor and previous shape based methods. While the previous method produces large image errors (Max. = 10.14, RMS = 3.0) (see Fig. 5(e)), our approach drastically reduces errors by about 80% (Max. = 1.92, RMS = 0.6) as seen in Figs. 5(c,f).

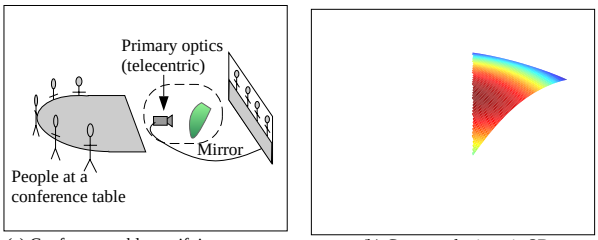

(a) Conference table rectifying system

(b) Computed mirror in 3D

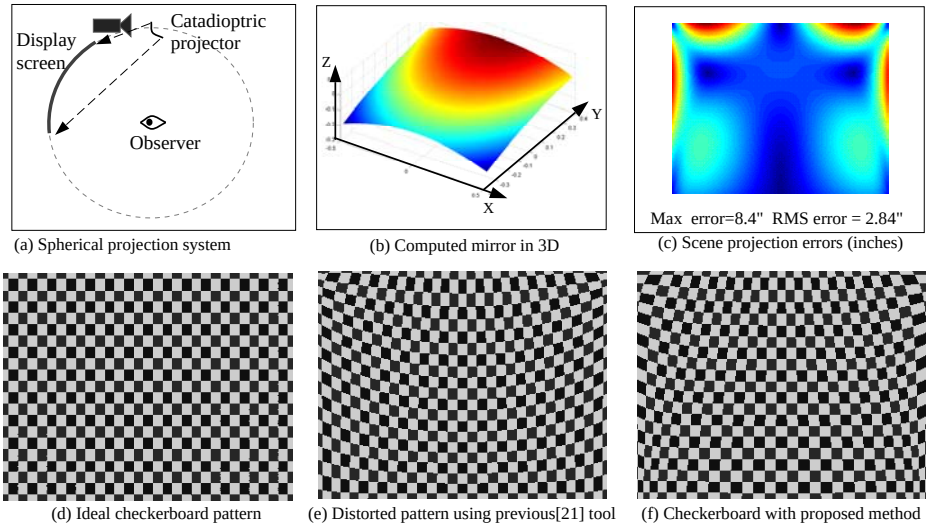

(a) Spherical projection system (b) Computed mirror in 3D (c) Scene projection errors (inches)

(d) Ideal checkerboard pattern (e) Distorted pattern using previous[21] tool (f) Checkerboard with proposed method

Figure 6. (a) A spherical immersive screen with the observer seated in the center. The projector is located on the roof and is expected to project a section of a spherical panorama on the screen as shown. (b) The mirror computed using our scene projection error minimizing approach. (c) Errors in projection onto the sphere are very small in comparison with the mirror shape error minimizing technique. (d) Ideal checkerboard pattern projected on the sphere. (e) Equivalent checkerboard pattern using the mirror shape error minimizing method showing stronger distortions. (f) Checkerboard pattern projected using our proposed method is visibly much lesser distorted.

known primary optics, we presented a method to compute the mirror shape by solving a linear set of equations.

Our method improves upon a previous linear method [21, 20] for mirror design. By modifying the linear constraints, we claim that the mirror solution thus obtained approximately minimizes image errors rather than errors in mirror shape. We first derived a first order approximation of the image and scene error. This approximation is used to compute an appropriate transformation that must be applied to the previous linear constraints. The mirror solution to this new set of transformed equations now minimizes image errors or scene projection errors as required. The advantage of our technique is that we still can solve for the mirror shape linearly (in under 15 minutes of runtime) without the need for costly and potentially unstable non-linear optimizations.

We have demonstrated the ability of our system to consistently outperform the prior general mirror design method. We have shown in some cases the decreases in distortion and increase in performance can be as much as 80%. Due to the often dramatic increased performance of a system using our method we believe our technique gives designers a new level of control and flexibility in creating catadioptric systems.

References

1. Rees, D.: Panoramic Television viewing System. United States Patent No.3,505,465 (1970)
2. Yagi, Y., Yachida, M.: Real-Time Generation of Environmental Map and Obstacle Avoidance Using Omnidirectional Image Sensor with Conic Mirror. In: Proc. CVPR. (1991) 160–165
3. Yamazawa, K., Yagi, Y., Yachida, M.: Omnidirectional Imaging with Hyperboloidal Projection. In: Proc. IEEE/RSJ International Conference on Intelligent Robots and Systems. (1993) 1029–1034
4. Nalwa, V.: A True Omnidirectional Viewer. Technical report, Bell Laboratories, Holmdel, NJ 07733, U.S.A. (1996)
5. Nayar, S.K.: Catadioptric Omnidirectional Cameras. In: Proc. CVPR. (1997) 482–488
6. Baker, S., Nayar, S.K.: A Theory of Catadioptric Image Formation. In: Proc. ICCV. (1998) 35–42
7. Chahl, J., Srinivasan, M.: Reflective Surfaces for Panoramic Imaging. Applied Optics **36** (1997) 8275–8285
8. Gaspar, J., Decco, C., Okamoto Jr, J., Santos-Victor, J.: Constant Resolution Omnidirectional Cameras. In: Proc. OMNIVIS. (2002) 27
9. Hicks, R., Perline, R.: Equi-areal Catadioptric Sensors. In: Proc. OMNIVIS. (2002) 13
10. Bogner, S.: Introduction to Panoramic Imaging. In: IEEE SMC Conference. Volume 54. (1995) 3100–3106
11. Derrien, S., Konolige, K.: Aproximating a Single Viewpoint in Panoramic Imaging Devices. In: ICRA. (2000) 3932–3939
12. Benosman, R., Deforas, E., Devars, J.: A New Catadioptric Sensor for the Panoramic Vision of Mobile Robots. In: Proc. OMNIVIS. (2000)
13. Hicks, R., Bajcsy, R.: Catadioptric Sensors that Approximate Wide-Angle Perspective Projections. In: Proc. CVPR. (2000) I:545–551
14. Gächter, S.: Mirror Design for an Omnidirectinal Camera with a Uniform Cylindrical Projection when using the SVAVISCA Sensor. Technical Report CTU-CMP-2001-03, Czech Technical University (2001)
15. Bruckstein, A., Richardson, T.: Omniview Cameras with Curved Surface Mirrors. In: Proc. OMNIVIS. (2000) 79–84
16. Marchese, F.M., Sorrenti, D.G.: Mirror Design of a Prescribed Accuracy Omnidirectional Vision System. In: Proc. OMNIVIS. (2002) 136
17. Hicks, A.: Differential Methods in Catadioptric Sensor Design with Applications to Panoramic Imaging. Technical report, Drexel University, Computer Science (2002)
18. Born, M., Wolf, E.: Principles of Optics. Permagon Press (1965)
19. Hecht, E.: OPTICS. Second edn. Addison-Wesley, Massachusetts (1987)
20. Halstead, M., Barsky, B., Klein, S., Mandell, R.: Reconstructing curved surfaces from specular reflection patterns using spline surface fitting of normals. In: Proc. SIGGRAPH. (1996) 335–342
21. Swaminathan, R., Nayar, S., Grossberg, M.: Framework for Designing Catadioptric Projection and Imaging Systems. In: Proc. ICCV-PROCAMS. (2003)
22. Grossberg, M., Nayar, S.: A General Imaging Model and a Method for Finding its Pa rameters. In: Proc. ICCV. (2001) 108–115
23. Nayar, S., Peri, V.: Folded Catadioptric Cameras. In: Proc. CVPR. (1999) II: 217–223